ORIGINAL ARTICLE

Influence of stacking sequence on mechanical properties and moisture absorption of epoxy-based woven flax and basalt fabric hybrid composites

Kehinde Olonisakin[a], Suping He[b], Yuefei Yang[c], Haopeng Wang[d], Ran Li[a,*], Wenbin Yang[a,*]

[a]College of Materials Engineering, Fujian Agriculture and Forestry University, Fuzhou, Fujian, China.

[b]Hua Xiangyuan Tea Industry Co. Ltd, Xiamen, Fujian, China.

[c]Xiamen Quality Inspection Institute, Xiamen, Fujian, China.

[d]Fujian Science and Technology Innovation Laboratory for Optoelectronic Information of China, Fuzhou, 350100, China.

[*]Corresponding Authors: Ran Li, szylr@163.com, Wenbin Yang, fafuywb@163.com.

Abstract: Hybrid composite laminates (HCL) were prepared by lay-up molding using a hot-press bed for reinforcing epoxy-based woven flax and basalt fabric composites. Mechanical properties and moisture absorption of HCL were measured, and the fracture surface was examined by scanning electron microscopy (SEM). The present results indicated that the mechanical properties of HCL are strongly dependent on the sequence of fiber reinforcement. HCL (S2, S3, S4, S5) with symmetric stacking sequences that increase with basalt fibers (wt %) showed a positive hybridization effect on mechanical properties and curve characteristics. However, the mechanical properties of S7 (asymmetric stacking) were lower than S3, S4, S5 (symmetric stacking), which indicated that symmetric stacking sequences of HCL had superior mechanical performance compared with the cross arrangement of HCL. The moisture absorption of HCL samples immersed in water at 26 ℃ showed the Fickian behaviour up to 42 days and were not affected by altering the stacking sequence on HCL. The SEM of the fracture surface, fiber-matrix bonding, and interfacial bonding of flax-basalt fabric HCL were also presented.

Keywords: Stacking sequence; woven flax; basalt fabric; composite; mechanical properties; water absorption

1. Introduction

Composite materials have gained growing interest in structural applications due to their improved performance as compared with single materials in the last few decades [1, 2]. Typically, hybrid composites consist of at least two fibers bonded together in a common matrix (**Fig. 1**). A hybrid composite can be created from an artificial-artificial, natural-artificial or natural-natural fiber combination. Consequently, new composite materials are developed with new and enhanced properties [3]. One of the most effective ways to achieve desirable properties in laminated composites is hybridization [4]. Unlike single-type fiber-reinforced composites, hybrid composites combine two or more types of fibers to provide superior properties [5]. Through hybridization, one can benefit from the advantages of various fibers and eliminate their weaknesses, and this can improve the fracture toughness, fatigue resistance, as well as reduce the overall cost or weight of composite laminates [6].

Because composite materials are low-cost, have a high strength-to-weight ratio, and are easy to manufacture, they have wide application in engineering. Natural fibers as reinforcement materials for polymeric composites has gained increased interest in recent years [7,8] due to their low costs, good mechanical properties, high strengths, non-abrasive properties, eco-friendliness and biodegradability [9-12]. Natural fibers, on the other hand, have lower mechanical properties than synthetic fibers, including carbon fibers, glass fibers, aramid fibers, and so on. Moreover, the disadvantage of natural fiber composites is the poor resistance to moisture absorption [11-14], hence, a stronger and stiffer fiber is introduced into hybrid composite laminates (HCL) to enhance mechanical properties and reduce moisture absorption.
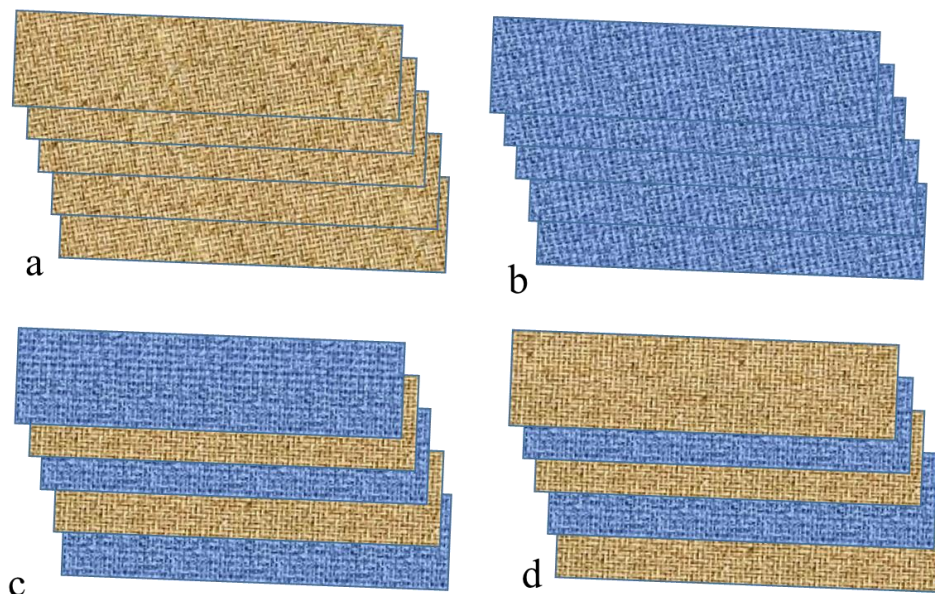
Fig. 1. a, b: single laminate composite and c, d: hybrid laminate composites

Basalt fiber is obtained from basaltic volcanic rocks. It is of research importance due to its excellent chemical stability, superior temperature resistance, higher strength, modulus, and better strain to failure than carbon fiber as an inorganic fiber [11]. It is non-toxicity, resistant to weather, and has non-combustibility properties [15-17]. Basalt fiber is environment-friendly, with good mechanical properties and easy processibility [11,18]. Basalt fiber has been used to reinforce military-grade composites, structural retrofitting and seismic reinforcement [19]. It is an excellent reinforcement material in composites when combined with other fibers [20-22].

As regards hybridization and stacking sequences, previous studies suggested that degradation patterns are most favorable with an asymmetric configuration including a low strength material (glass) in the core of a high strength material (basalt) [23]. The fibers of the basalt fabric as the core and the glass fabric as the outer layer were reported to have high tensile strength reaching 356.39 MPa in composite reinforced with glass fiber fabric and basalt fabric with sandwich stacking sequence configuration [24]. One study suggested that external basalt fiber layers result in the greatest enhancement of flexural and tensile properties among various stacking sequences of glass/basalt [25]. In composites fabricated with alternate layers of basalt fiber and jute fiber, different layering patterns influence the tensile and flexural properties [26]. The stacking order provided higher strength in basalt/glass fiber intercalated hybrid laminates composite [24,26]. Basalt and jute fibers in an epoxy bio-based hybrid composite showed that inter-ply hybridization resulted in better mechanical properties from their stacking sequences [24,27].

In addition to basalt fibers, some researchers have used jute fibers, nylon, woven fabrics, and aluminum fibers as reinforcements in HCL structures [28,29], etc. Flax fiber is becoming increasingly promising as co-reinforcement in polymer composite due to its commercial availability, low cost and specific mechanical properties [30]. Many studies have reported on flax fiber-reinforced composites. For instance, it has been used as co-reinforcement in carbon and flax fabric reinforced hybrid

composites [31], pineapple leaf-flax reinforced hybrid composite [32], as reinforcement in polyamide 11 resin [33], and Flax/Jute epoxy-based composites [14]. The effect of stacking sequence and hybridization on the properties of the hybrid composite material has only been assessed in a limited amount of studies involving flax fibers and basalt fibers. Hybridizing flax fibers with basalt fibers would reduce costs and increase the application scope of composite materials [34].

As a result of the above considerations, flax and basalt fabrics were used as reinforcements in epoxy resin matrix for HCL. This study examines how different stacking sequences affect woven flax and basalt fabrics' mechanical properties and water absorption.

The objective is to investigate the effect of different stacking sequences on the mechanical properties and water absorption of the woven flax and basalt fabric HCL.

2. Experimental

2.1 Materials

Flax fabric having a count of 22×12 (22 yarns of Tex 310 in the warp direction and 12 yarns of Tex 280 in the weft direction, per inch) was obtained from Xin Shen group Co. Ltd. (Wujiang, China). The weight of the fabric was approximately 168 g/m². Basalt fiber fabrics of a weight of 200 g/m² were supplied by Dongguan Gold Basalt Fiber Co. Ltd. (Dongguan, China). A mixture of epoxy (E-44) having modified aliphatic amine hardener was supplied by Zhengjiang Resins Industry (Zhengjiang, China) was the matrix. The properties of the woven flax, basalt fiber fabric, and epoxy resin properties respectively are presented in **Tables 1** and **Tables 2**.

Table 1. Properties of the woven flax and basalt fabric

Properties	Flax fabric	Basalt fabric
Filament diameter (μm)	/	7
Fabric weight (g/m²)	168	200
Fabric thickness (mm)	0.3	0.18
Yarn count	22×12	/
Style	Plain weave	Plain weave

Table 2. Properties of the epoxy resin (E-44)

Properties	Epoxy resin (E-44)
Specific gravity (25 ℃)	1.18 g/cm³
Viscosity (Pa s, 25 ℃)	6-10
Softening point (℃)	12-20
Hardener	Polyamide

2.2 Fabrication of HCL

(a)   (b)
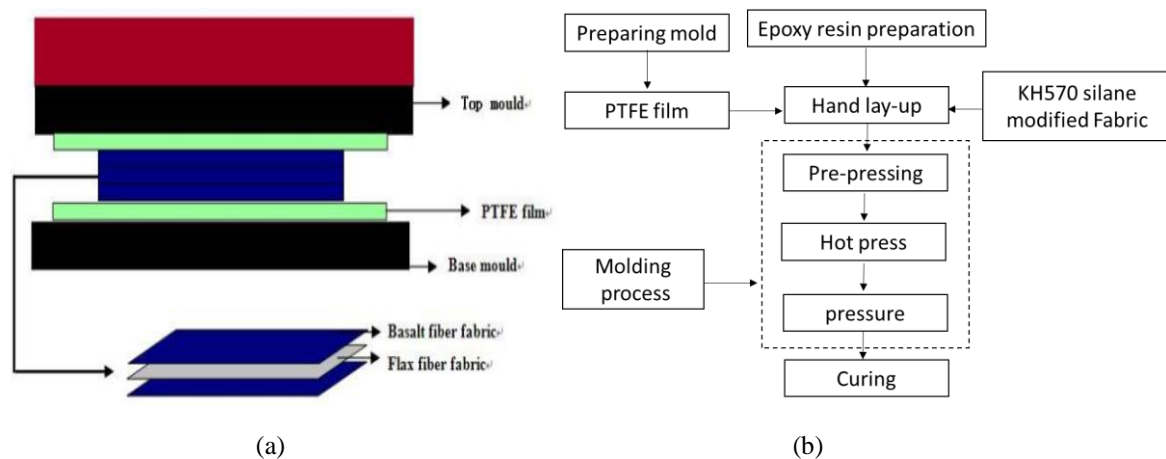
Fig. 2. (a) Schematic representation of composite fabrication. (b) The fabrication process of HCL.

The HCL series were fabricated manually using a hot press. The flowchart is shown in **Fig.2**(a) and **Fig.2**(b). Polytetrafluoroethylene (PTFE) film was applied to the surface of the mold. Woven basalt and flax fabric, cut to 220 mm × 220 mm, modified with silane coupling agent KH570 (G-570, γ-methacryloxypropyltrimethoxysilane) in 80/10 volume ethanol/water. The modified fiber was then stacked on a stainless plate mold (250 mm × 250 mm) in different sequences. The epoxy resin was brushed on to the flax and basalt fabrics (1:1 epoxy/hardener) and pressed in the mold for 6 minutes (5 MPa) before being removed. The mold was designed to allow hot gases to escape. We used spacers of the desired thickness to achieve uniform thickness on the mold plates. After 6 min, the HCL was removed from cold press and then cured for 40 min at 110 ℃ and 8 MPa, respectively. Then the HCL was removed from the hot press and cooled with the pressure at 5 MPa for 60 min at room temperature. Finally, the HCL was removed from the mold for characterization.

Table 3. Laminate stacking sequence

Symbol	Stacking sequence	Flax	Basalt	Total fiber (flax + basalt)		Thickness (mm)
		Weight fraction (%)		Weight fraction (%)	Volume Fraction (%)	
All flax fiber (S1)	F10	100	0	33.3	31.3	3.15
1 symmetric basalt layers (S2)	F8B2	77	23	33.3	32.1	3.16
2 symmetric basalt layers on both outer layer (S3)	F6B4	55	45	33.5	33.0	3.03
3 symmetric basalt layers on both outer layer (S4)	F4B6	39	61	33.3	33.2	3.00
4 symmetric basalt layers on both outer layer (S5)	F2B8	19	81	33.3	34.1	2.96
All basalt layers(S6)	B10	0	100	33.3	34.7	3.20
Alternate asymmetric basalt/flax layer (S7)	B5F5	49	51	33.3	33.2	3.03

Note: F-flax ply, B-basalt ply
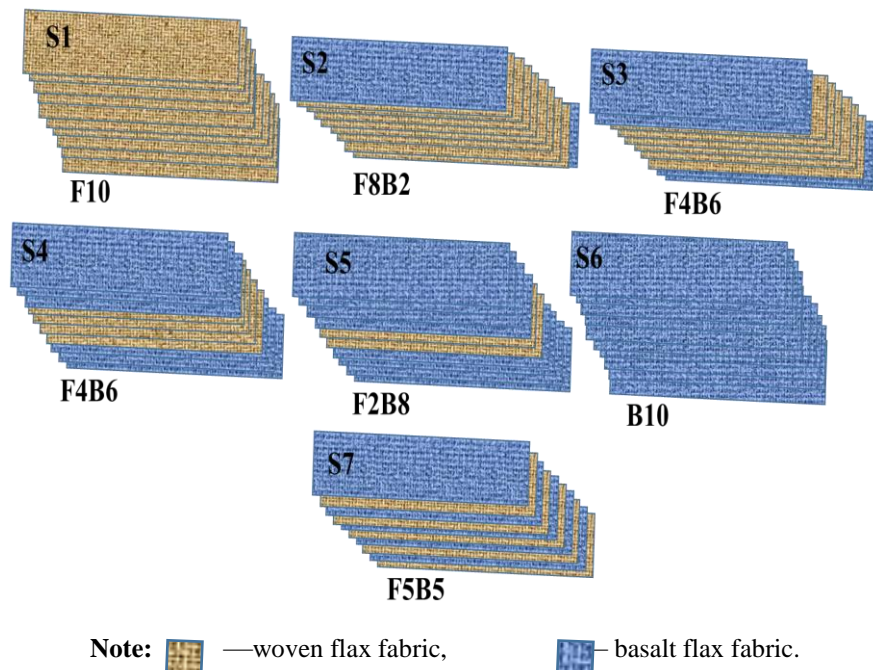
Note: ▨ ——woven flax fabric, ▨ – basalt flax fabric.
Fig. 3. Stacking sequences of woven flax (F), basalt (B) fabric.

For the present investigation, woven flax and basalt fabrics were stacked between ten layers in each composite laminate configuration consisting of flax, basalt and epoxy. Based on the arrangements in **Fig. 3**, we designed different woven flax, and basalt fabric layers to study the effect

of stacking sequences. In each panel of HCL, flax and basalt fabrics made up 33.3 wt% of the weight as shown in **Table 3**. The total fiber volume fraction is calculated using Eq. (1):[35]

$$V_{\text{f}} = \frac{(W_{\text{f}} / \rho_{\text{f}}) + (W_{\text{b}} / \rho_{\text{b}})}{(W_{\text{f}} / \rho_{\text{f}}) + (W_{\text{b}} / \rho_{\text{b}}) + (W_{\text{r}} / \rho_{\text{r}})} \tag{1}$$

W_{f}, W_{b} and W_{r} are the weights of the flax, basalt and resin, respectively. ρ_{b}, ρ_{f} and ρ_{r} are the densities of basalt, flax and density of resin, respectively. The density of epoxy resin is 1.18 g/cm^3, as provided by the manufacturer. The density of basalt and flax are about 200 g/m^3 and 168 g/m^3, respectively. Both of them were taken from the supplier's datasheet.

2.3 Characterization

Tests for tensile strength, flexural strength, impact strength, and water absorption were carried out according to ISO 527-4 (test conditions for fiber-reinforced plastic composites), ISO 14125 (plastic composites-determination of flexural properties), and ISO 179-1 (plastics-determination of Charpy impact properties, and ASTMD570, respectively).

2.3.1 Tensile test

A diamond wheel saw was used to carefully cut out pieces of laminate for the tensile test before finishing to the correct size with emery paper. The dimensions of the test specimen are 180 mm by 20 mm by 3 mm. The tests were conducted on an MTS Systems CMT6104 microcomputer controlled electronic universal testing machine (SHENZHEN, China). The load applies was 50 kN and a gauge length of 50 mm. A rate of loading of 10 mm/min was used for testing. The tensile strength (σ_{t}) of the HCL was determined according to Eq. (2).

$$\sigma_{\text{t}} = \frac{F}{bd} \tag{2}$$

Where F, b and d represent the fracture load, specimen width, and specimen depth. Five replicate specimens were tested for each stacking sequence, and the average result was used for the report.

2.3.2 Flexural test

Samples length and width of 70 and 15 mm were cut from laminate for the three-point bending with a span to depth ratio of 16:1. The test was conducted at a loading rate of 5 mm/min and load of 10 kN. The flexural strength (σ_{F}) and flexural modulus (E_{F}) of the HCL were determined using Eq. (3) and Eq. (4).

$$\sigma_{\text{F}} = \frac{3PL}{2bd^2} \tag{3}$$

$$E_{\text{F}} = \frac{L^3 m}{4bd^3} \tag{4}$$

Where L, b, d, P and m are the support span, width, depth, load, and the initial slope of the load-displacement curve, respectively. For each stacking sequence, five parallel measurements were performed.

2.3.3 Impact test

The unnotched specimens were used for the Impact tests with a length, width, and thickness of 80 mm, 10 mm and 4 mm respectively, and tested on a ZBC-25B Charpy Impact Tester (MTS System, Guangdong, China). The impact strength (acU) of the HCL was determined according to Eq. (5).

$$acU = \frac{E_{\text{c}}}{hb} \times 10^3 \tag{5}$$

Where E_{c}, h and b represent, the test specimen's absorbed energy, thickness, and width. Five samples were tested for each case of stacking sequence.

2.3.4 Moisture absorption test

Samples of 76.2 mm (3 in.) long and 25.4 mm (1 in.) wide were used for the moisture absorption. After preconditioning at 70 ℃ for 24 hours, all samples were weighed accurately to 0.0001 g in an electronic balance with a single precision, cooled in desiccators, and weighed immediately (m_1), and the samples were placed back in water. The samples were immersed in a water bath at 26 ℃ for each group of five samples. During the next 24 h, the samples were removed, the surface water was wiped off and the samples were weighed (m_2), after that, the samples were immersed again in water bath at 26 ℃. This procedure was repeated until the samples reached saturated point. The weight gained by the samples was carefully monitored. During the first week, the weight was checked everyday (24 h), then once a week for one month, and then once every two weeks until saturation was reached. This helped to closelt monitor the sample's weight gain. During this period, the water was changed regularly until saturation. The moisture absorption of the HCL was determined according to Eq. (6).

$$m_0 = \frac{m_2 - m_1}{m_2} \times 100\% \tag{6}$$

Where m_0, m_1 and m_2 represent the moisture absorption, conditioned weight, and wet weight.

2.3.5 Morphology of fracture surfaces

The fracture surface of the specimens was investigated using a scanning electron microscope (Nova Nanosem 230). All samples were sputtered with gold before SEM analysis.

2.3.6 Data analysis

Statistical analysis of mechanical properties was performed with SPSS 19 (IBM Corp., USA) using a one-way ANOVA at a 95% confidence interval.

3. Results and Discussion

3.1 Tensile properties

The changes in tensile strength and modulus for various laminates are shown in **Fig. 4**(a). The tensile strength and modulus of S6 (woven basalt fabric) are 212% and 483%, respectively, greater than S1 (woven flax fabric). The inclusion of basalt fiber as extreme basalt plies increased the tensile strength of the composite (S2, S3, S4, S5 and S6). Munikenche et al. [36] reported that the strength and modulus fibers has significant effect on the tensile strength of composites. According to the Rule of Mixture (ROM), Eq. (7) is given:

$$E_c = E_f \cdot V_f + E_m \cdot V_m \tag{7}$$

Where E_c, E_f and E_m are the moduli of composites, fibers and matrix, respectively. As a result, the hybrid composite had greater tensile and modulus strength due to basalt fibers having a higher strength and stiffness than flax fibers [37]. Compared to S1, the tensile strength and modulus of S5 (Flax fibers accounted for 19% of the total fibers) increased 154% and 417% respectively. **Fig. 4**(a) revealed that the HCL increases in tensile strength and modulus with the increase in basalt fiber content from 23% to 81% of the total fibers. The addition of glass fibers to jute fiber composites in isophthalic polyester in a previous study improved the tensile strength and tensile modulus of the composites [38]. At the same time, different stacking sequences on HCL can affect the mechanical properties. We observed that the tensile strength and tensile modulus of S7 were lower than those of S3. Interestingly, the proportion of basalt fibers in S7 (51%) is higher than in S3 (45%). The reason may be ascribed to the uneven loading of asymmetric stacking sequence of S7 to speed up the failure process of tensile fracture.

A correlation equation between tensile strength (MPa) and basalt fibers contents (wt %) is established in **Fig. 4**(b). The equation (y=0.0068x^2+0.7005x+57.556) was obtained through numerical results simulation and regression analysis, with a high correlation coefficient (R^2=0.95552). The initial slopes of S1, S2, S3, S4, S5, and S6 show a non-linear pattern.

3.2 Flexural properties

The averaged flexural strength and modulus of the HCL are shown in **Fig. 4**(c). The flexural strength and modulus of S6 rank at the top, 111% and 222% higher than S1. The flexural strength and modulus of S5 are 173 MPa and 10.7 GPa, which is 57% and 49% higher than S2, respectively. Flexural strength and modulus of HCL are increased with the basalt fibers content from 23% to 81% of the total fiber weight. The initial slopes of S1, S2, S3, S4, S5, and S6 show a steep increase in **Fig. 4**(d). The corresponding two-order polynomial equation ($y=0.0004x^2+0.585x+97.27$) and R^2 (0.9895) were obtained. No improvement in flexural properties was observed by altering the arrangement sequence, as was the case for S7. Among the HCL (S3, S4, S5), S7 has the lowest flexural strength (128 MPa) and modulus (7.8 GPa), similar to that of S3. These findings are in line with the findings of [29,39] that the modulus and flexural strength of HCL were strongly affected by the sequence of fiber reinforcement.

Note: S1 and S6 represent all flax and basalt laminates, respectively. The rest means HCL with woven flax and basalt fabric.

(a)　　　　　　　　　　　　　　(b)

(c)　　　　　　　　　　　　　　(d)
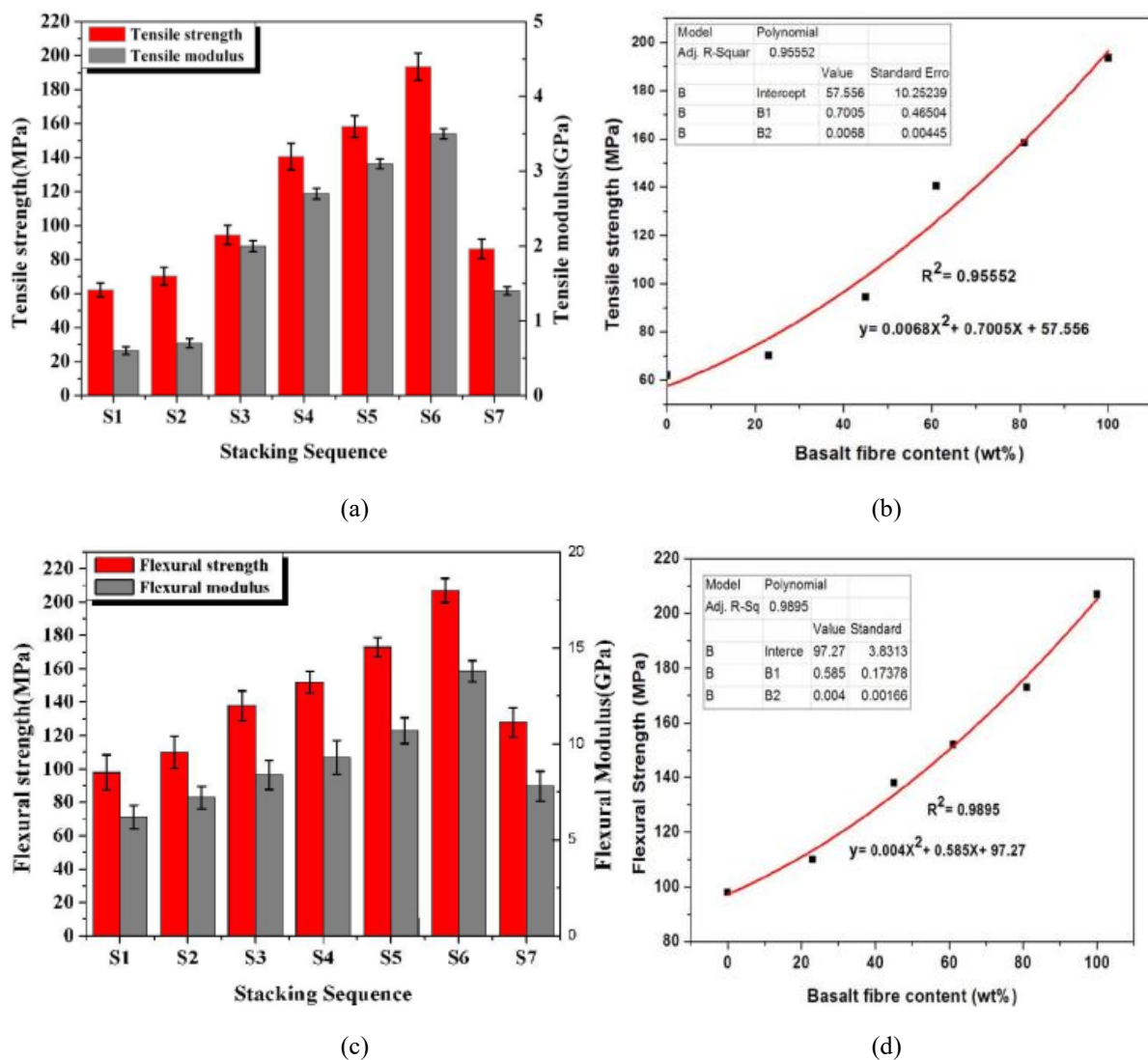
Fig. 4. Effect of stacking sequences on the tensile strength and tensile modulus (a), flexural strength and modulus (b), fitted curve of tensile strength vs basalt fiber content (c), fitted curve of flexural strength vs basalt fiber content (d).

3.3 Impact properties

S5 has the highest impact strength of 167.4 kJ/m^2, (**Fig. 5**(a)), 71% and 86% higher than S1 and

S2, respectively. The impact strength of laminates gradually increased from S1 to S6, and this phenomenon agrees with the results of tensile and flexural properties presented in **Fig. 5**(b). The polynomial (y=-0.045x^2+1.33595x+83.1747) and R^2 (0.90584) were obtained by curve-fitting impact strength versus basalt fiber content. According to the studies of Dehkordi et al. [3], which examined the impact properties of intra-ply hybrid composites based on nylon and basalt fibers, the number of basalt fibers in these composites significantly affected the impact performance. Although S7 contains more basalt fiber (wt%) than S3, its impact properties is much lower than S3. Higher impact strength is due to the basalt fiber arrangement on both sides of the HCL. Hence it is difficult for cracks to propagate. Fiber stacking sequence is highly important to HCL, whose layers have different fiber types [23].

(a)   (b)
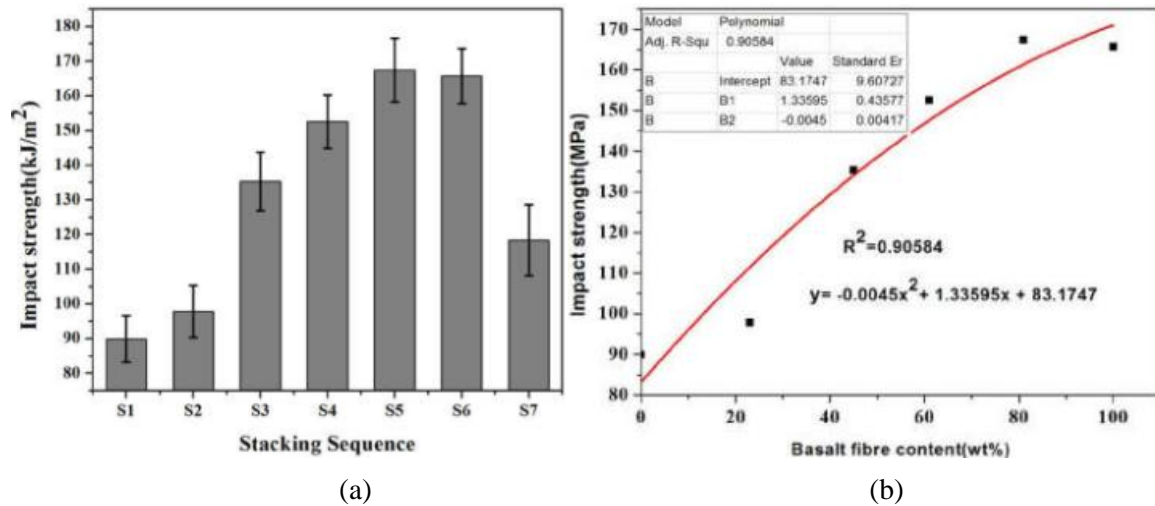
Fig. 5. Effect of different stacking sequences on the impact strength (a), the fitted curve of impact Strength vs basalt fiber content (b).

3.4 Moisture absorption

(a)   (b)
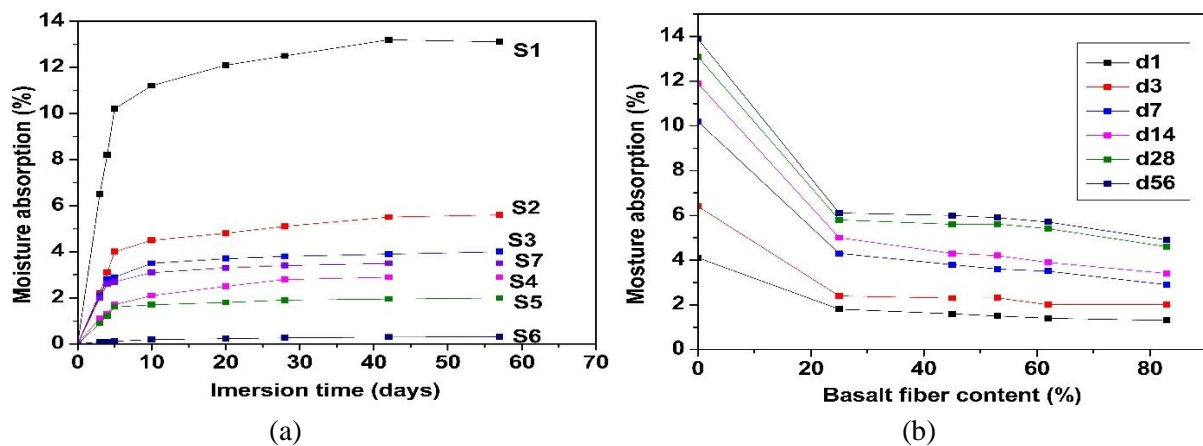
Fig. 6. Effect of different stacking sequences on water absorption of HCL. (a) Percentage of moisture absorption vs immersing time. (b) Percentage of moisture absorption vs basalt fiber weight fraction for different immersion time

The moisture absorption curves of HCL are shown in **Fig. 6**(a). Every point is the average of five data sets. There was a linear portion to the curves initially, but all composites reached saturation after 42 days of immersion and showed a typical Fickian behavior. During the early phase of immersion, the water absorption of natural fiber composites increased linearly according to Fickian law [40], the composites in this study follow this law. S1 has the highest moisture absorption in all the composites. The optimum moisture absorption of S1, S2, S3, S4, S5 and S7 were 13.72%, 5.72%, 4.87%, 4.68%, 4.11% and 3.44%. The moisture absorption of S6 HCL was lower than all the HCL. The reason is that basalt fiber is an inorganic and hydrophobic material consisting of metallic oxides, such as SiO$_2$,

Al_2O_3, FeO, Fe_2O_3, MgO, K_2O, Na_2O and so on [15]. In this way, basalt fiber acts as a barrier and prevents direct contact between flax and water. **Fig. 6**(b) shows that adding woven basalt fabrics to extreme surfaces reduces moisture absorption considerably for various immersion times. Flax is highly hydrophilic nature and is accountable for the high moisture absorption in all composites. By altering the sequence of arrangement in S7, no change in the water absorption was found, similar to the case of S3. It was revealed that the water absorption of woven flax and basalt fabric HCL was associated with the type and proportion of the fiber rather than the stacking sequence.

3.5 Morphology of fracture surfaces

Each fiber within a composite laminate has a unique fracture characteristic, such as fiber pull-out, breakage, debonding, etc. Failure of a laminate depends on the maximum bending moment the fibers in the laminate can handle. To provide insight into how the samples are damaged following flexural testing, optical and scanning electron microscope images were captured of the front and fractured surfaces of the samples. Flax fibers were pulled out and fractured from **Fig. 7** (A and A1). S1 shows poor interfacial adhesion between fiber and matrix. When basalt fiber layers are sandwiched between the top and bottom of the flax fiber layers, for S5, no basalt fiber was pulled out, and the matrix was not destroyed (**Fig. 7**(B)). This may be due to basalt fiber's higher strength and modulus than flax fiber [33]. A closer look in **Fig. 7** (B1 and B2) reveals a few defects, such as debonding and cracks between flax fibers and matrix. The reason is that basalt fibers of the outer layer have absorbed most of the applied load, resulting in the protection of the flax layer. For the basalt/epoxy composites, fiber fracture and matrix fragment were observed in **Fig. 7**(B1), indicating that the crack of the matrix under the external force resulted in the collapse of the composites. S6 shows that the interfacial adhesion between basalt fiber and matrix is better than between flax fiber and matrix, as shown in **Fig. 7**(C). So the S6 has the highest mechanical performance.
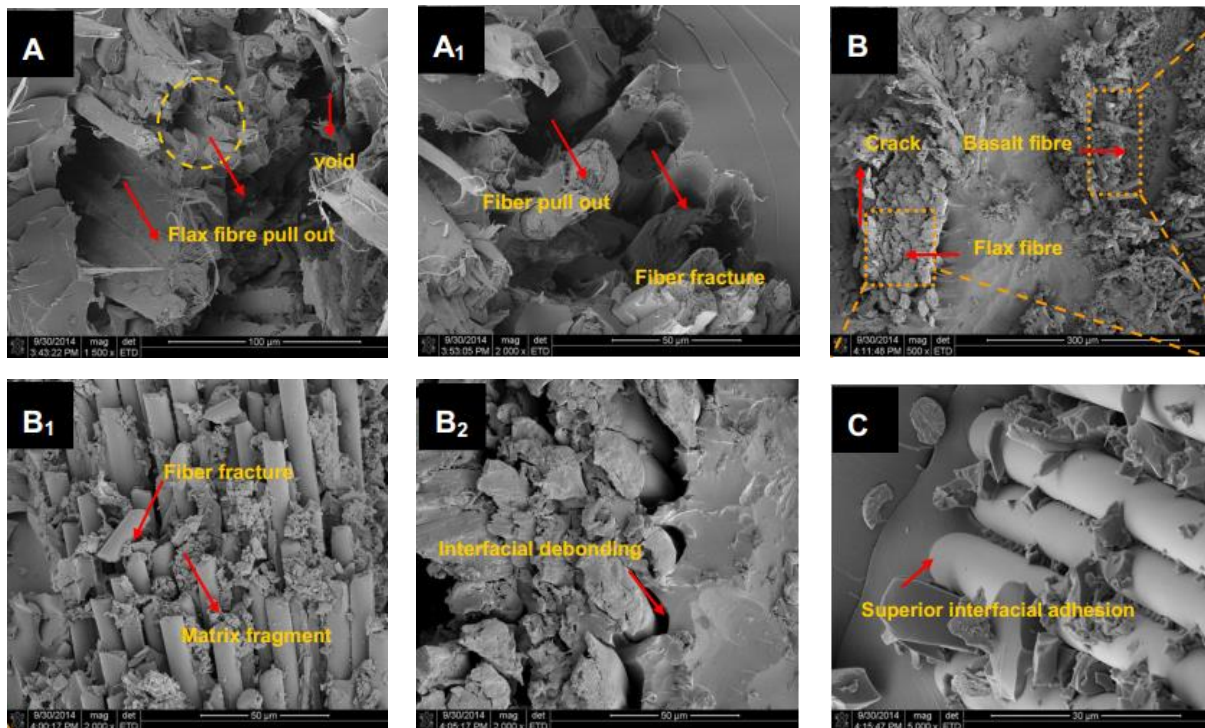
Fig. 7. SEM images of the cross-section of the fractured surfaces of flax fibers S1 (A and A1), flax and basalt fibers S5 (B, B1 and B2), basalt fibers S6 (C).

4. Conclusions

Based on the results from this study, it can be concluded that:

(1) Incorporation of basalt fabric in flax fabric HCL improved the mechanical properties and resistance to moisture absorption of the epoxy-based woven flax and basalt fabric composites.

Altering the stacking sequence significantly affects the mechanical properties of HCL but does not affect moisture absorption.

(2) For the similar relative weight fraction of woven flax and basalt fabric, symmetric stacking sequences of HCL have superior mechanical performance compared with the cross arrangement of HCL.

(3) Moisture-absorption of woven flax and basalt HCL samples immersed in water at 26 ℃ follows the Fickian behaviour up to 42 days. The moisture saturation level of flax composites (S1) was 13.72%, which decreases with the increase of basalt fabric. An addition of 81% basalt fiber in HCL decreases the moisture saturation to 4.11% after 42 days.

(4) Fractography of the fractured surfaces of flax composites (S1) reveals a poor adhesion between the woven flax fibers and the matrix. However, basalt composites (S6) have an excellent interfacial bond between fibers and matrix.

Acknowledgements

CRediT authorship contribution statement

Kehinde Olonisakin: Data curation, Investigation, review & editing, **Suping He**: Software, Visualization, **Yuefei Yang**: Original draft, Methodology, review, **Haopeng Wang**: Software, Formal analysis, **Ran Li**: review & editing, Validation, **Wenbin Yang**: Supervision, Project administration, funding acquisition.

Authors Statement

The authors declare no conflict of interest.

References

[1] Tehrani Dehkordi M, Nosraty H, Shokrieh MM, Minak G, Ghelli. Influence of hybridization on impact damage behavior and residual compression strength of intraply basalt/nylon hybrid composites. Materials & Design 2013; 43: 283-290. https://doi.org/10.1016/j.matdes.2012.07.005.

[2] Ömer Yavuz Bozkurt ÖÖ, Bulut Mehmet. The Influence of Fiber Orientation Angle on Damping and Vibration Properties of Basalt Fiber Reinforced Composite Laminates. Journal of Civil, Structural and Transportation Engineering (JCSTE) 2016; 2: 12-16.

[3] Dehkordi MT, Nosraty H, Shokrieh MM, Minak G, Ghelli D. Low velocity impact properties of intra-ply hybrid composites based on basalt and nylon woven fabrics. Materials & Design 2010; 31(8): 3835-3844. https://doi.org/10.1016/j.matdes.2010.03.033.

[4] Khoramishad H, Mousavi MV. Hybrid polymer composite materials. The 7th International Conference on Applied Science and Technology (Icast 2019), 2019. Engineering 2014; 58: 251-258. https://doi.org/ 10.10 63/1.5123100.

[5] Safri SNA, Sultan MTH, Jawaid M, Jayakrishna K. Impact behaviour of hybrid composites for structural applications: A review. Composites Part B: Engineering 2018; 133: 112-121. https://doi.org/ 10.1016/j.com positesb.2017.09.008.

[6] Sevkat E, Liaw B, Delale F. Ballistic performance of hybrid and non-hybrid composite plates. The Journal of Strain Analysis for Engineering Design 2012; 47(7): 453-470. https://doi.org/ 10.1177/03093247124578 97.

[7] Sakakibara K, Rosenau T. Polythiophene-cellulose composites: synthesis, optical properties and homogeneous oxidative co-polymerization %J 2012; 66(1): 9-19. https://doi.org/10.1515/HF.2011.137.

[8] Wu TL, Chien YC, Chen T-Y, Wu J-H. The influence of hot-press temperature and cooling rate on thermal and physicomechanical properties of bamboo particle-polylactic acid composites. Holzforschung 2012; 67(3): 325-331.

[9] Rana AK, Mandal A, Bandyopadhyay S. Short jute fiber reinforced polypropylene composites: effect of compatibiliser, impact modifier and fiber loading. Composites Science and Technology 2003; 63(6): 801-806. https://doi.org/10.1016/S0266-3538(02)00267-1.

[10] Dweib MA, Hu B, O'Donnell A, Shenton HW, Wool RP. All natural composite sandwich beams for structural applications. Composite Structures 2004; 63(2): 147-157. https://doi.org/10.1016/S0263-8223(03)00143-0.

[11] Abd El-Baky MA, Attia MA, Abdelhaleem MM, Hassan MA. Flax/basalt/E-glass Fibers Reinforced Epoxy Composites with Enhanced Mechanical Properties. Journal of Natural Fibers 2020; 19(3): 954-968. https://doi.org/10.1080/15440478.2020.1775750.

[12] Abd El-baky MA, Attia MA, Abdelhaleem MM, Hassan MA. Mechanical characterization of hybrid composites based on flax, basalt and glass fibers. Journal of Composite Materials 2020; 54(27): 4185-4205. https://doi.org/10.1177/0021998320928509.

[13] Caprino G, Carrino L, Durante M, Langella A, Lopresto V. Low impact behaviour of hemp fibre reinforced epoxy composites. Composite Structures 2015; 133: 892-901. https://doi.org/10.1016/j.compstruct.2015.08.029.

[14] Fiore V, Calabrese L. Effect of Stacking Sequence and Sodium Bicarbonate Treatment on Quasi-Static and Dynamic Mechanical Properties of Flax/Jute Epoxy-Based Composites. Materials (Basel) 2019; 12(9). https://doi.org/10.3390/ma12091363.

[15] Lopresto V, Leone C, De Iorio I. Mechanical characterisation of basalt fibre reinforced plastic. Composites Part B: Engineering 2011; 42(4): 717-723. https://doi.org/10.1016/j.compositesb.2011.01.030.

[16] Wei B, Cao H, Song S. Degradation of basalt fibre and glass fibre/epoxy resin composites in seawater. Corrosion Science 2011; 53(1): 426-431. https://doi.org/10.1016/j.corsci.2010.09.053.

[17] Wang X, Wu Z, Wu G, Zhu H, Zen F. Enhancement of basalt FRP by hybridization for long-span cable-stayed bridge. Composites Part B: Engineering 2013; 44(1): 184-192. https://doi.org/10.1016/j.compositesb.2012.06.001.

[18] Iyer NP, Arunkumar N. Dynamic analysis of hybrid basalt and carbon fiber reinforced Bismaleimide composites suited for high temperature structural applications. Materials Research Express 2021; 8(12). https://doi.org/10.1088/2053-1591/ac3f0b.

[19] Wu Z, Wang X, Iwashita K, Sasaki T, Hamaguchi Y. Tensile fatigue behaviour of FRP and hybrid FRP sheets. Composites Part B: Engineering 2010; 41(5): 396-402. https://doi.org/10.1016/j.compositesb.2010.02.001.

[20] Chen D, Sun G, Meng M, Jin X, Li Q. Flexural performance and cost efficiency of carbon/basalt/glass hybrid FRP composite laminates. Thin-Walled Structures 2019; 142: 516-531. https://doi.org/10.1016/j.tws.2019.03.056.

[21] Ribeiro F, Sena-Cruz J, Branco FG, Júlio E. Hybrid FRP jacketing for enhanced confinement of circular concrete columns in compression. Construction and Building Materials 2018; 184: 681-704. https://doi.org/10.1016/j.conbuildmat.2018.06.229.

[22] Ferrante L, Sarasini F, TirillòJ, Lampani L, Valente T, Gaudenzi P. Low velocity impact response of basalt-aluminium fibre metal laminates. Materials & Design 2016; 98: 98-107. https://doi.org/10.1016/j.matdes.2016.03.002.

[23] Vijaya Ramnath B, Junaid Kokan S, Niranjan Raja R, Sathyanarayanan R, Elanchezhian C, Rajendra Prasad A, Manickavasagam VM. Technical Report. Materials and Design 2013; 51(Complete): 357-366. https://doi.org/10.1016/j.matdes.2013.03.102.

[24] Berkay KARAÇOR MÖ. Effect of Various Matrix Materials on Mechanical Properties of Basalt/Jute/Glass Fiber Reinforced Hybrid Composites. Çukurova Üniversitesi Mühendislik Fakültesi Dergisi 2021; 36(4): 941-954.

[25] Fiore V, Di Bella G, Valenza A. Glass–basalt/epoxy hybrid composites for marine applications. Materials and Design 2011; 32(4): 2091-2099. https://doi.org/10.1016/j.matdes.2010.11.043.

[26] Sarasini F, TirillòJ, Valente M, Valente T, Cioffi S, Iannace S, Sorrentino L. Effect of basalt fiber hybridization on the impact behavior under low impact velocity of glass/basalt woven fabric/epoxy resin composites. Composites Part A: Applied Science and Manufacturing 2013; 47: 109-123. https://doi.org/10.1016/j.compositesa.2012.11.021.

[27] Fiore V, Scalici T, Badagliacco D, Enea D, Alaimo G, Valenza A. Aging resistance of bio-epoxy jute-basalt hybrid composites as novel multilayer structures for cladding. Composite Structures 2017 160(C): 1319-1328. https://doi.org/10.1016/j.compstruct.2016.11.025.

[28] Tehrani-Dehkordi M, Nosraty H, Rajabzadeh Mh. Effects of plies stacking sequence and fiber volume ratio on flexural properties of basalt/nylon-epoxy hybrid composites. Fibers and Polymers2015; 16(4): 918-925. https://doi.org/10.1007/s12221-015-0918-8.

[29] Amuthakkannan P, Manikandan V, Jappes JTW, Uthayakumar M. Influence of stacking sequence on mechanical properties of basalt-jute fiber-reinforced polymer hybrid composites. Journal of Polymer Engineering 2012; 32(8-9): 547-554. https://doi.org/10.1515/polyeng-2012-0063.

[30] Yan L, Chouw N, Jayaraman K. Flax fibre and its composites – A review. Composites Part B: Engineering 2014; 56: 296-317. https://doi.org/10.1016/j.compositesb.2013.08.014.

[31] Wang A, Wang X, Xian G. The influence of stacking sequence on the low-velocity impact response and damping behavior of carbon and flax fabric reinforced hybrid composites. Polymer Testing 2021; 104. https://doi.org/10.1016/j.polymertesting.2021.107384.

[32] Kumar S, Saha A. Effects of stacking sequence of pineapple leaf-flax reinforced hybrid composite laminates on mechanical characterization and moisture resistant properties. Proceedings of the Institution of Mechanical Engineers, Part C: Journal of Mechanical Engineering Science 2021; 236(3): 1733-1750. https://doi.org/10.1177/09544062211023105.

[33] Lebaupin Y, Hoang TQT, Chauvin M, Touchard F. Influence of the stacking sequence on the low-energy impact resistance of flax/PA11 composite. Journal of Composite Materials 2019; 53(22): 3187-3198. https://doi.org/10.1177/0021998319837339.

[34] Artemenko SE, Kadykova YA. Polymer composite materials based on carbon, basalt, and glass fibres. Fibre Chemistry 2008; 40(1): 37-39. https://doi.org/10.1007/s10692-008-9010-0.

[35] Mallick PK. Fiber-Reinforced Composites Materials. Manufacturing, and Design, 3rd Edition ed., CRC press, Boca Raton 2007. https://doi.org/10.1063/1.5123100.

[36] Munikenche Gowda T, Naidu ACB, Chhaya R. Some mechanical properties of untreated jute fabric-reinforced polyester composites. Composites Part A: Applied Science and Manufacturing 1999; 30(3): 277-284. https://doi.org/10.1016/S1359-835X(98)00157-2.

[37] Jawaid M, Abdul Khalil HPS. Cellulosic/synthetic fibre reinforced polymer hybrid composites: A review. Carbohydrate Polymers 2011; 86(1): 1-18. https://doi.org/10.1016/j.carbpol.2011.04.043.

[38] Ahmed KS, Vijayarangan S. Tensile, flexural and interlaminar shear properties of woven jute and jute-glass fabric reinforced polyester composites. Journal of Materials Processing Technology 2008; 207(1): 330-335. https://doi.org/10.1016/j.jmatprotec.2008.06.038.

[39] Ary Subagia IDG, Kim Y, Tijing LD, Kim CS, Shon HK. Effect of stacking sequence on the flexural properties of hybrid composites reinforced with carbon and basalt fibers. Composites Part B: Engineering 2014; 58: 251-258. https://doi.org/10.1016/j.compositesb.2013.10.027.

[40] Petroudy SRD. Physical and mechanical properties of natural fibers. Advanced High Strength Natural Fibre Composites in Construction. Woodhead Publishing 2017; pp: 59-83.   https://doi.org/ 10.1016/B978-0-08-100411-1.00003-0.